QUANTUM CHEMISTRY

Observation of an isomerizing double-well quantum system in the condensed phase

Jascha A. Lau[1,2], Arnab Choudhury[1,2], Li Chen [2]*, Dirk Schwarzer[2], Varun B. Verma[3], Alec M. Wodtke[1,2,4]†

Molecular isomerization fundamentally involves quantum states bound within a potential energy function with multiple minima. For isolated gas-phase molecules, eigenstates well above the isomerization saddle points have been characterized. However, to observe the quantum nature of isomerization, systems in which transitions between the eigenstates occur—such as condensed-phase systems—must be studied. Efforts to resolve quantum states with spectroscopic tools are typically unsuccessful for such systems. An exception is CO adsorbed on NaCl(100), which is bound with the well-known OC–Na^+ structure. We observe an unexpected upside-down isomer (CO–Na^+) produced by infrared laser excitation and obtain well-resolved infrared fluorescence spectra from highly energetic vibrational states of both orientational isomers. This distinctive condensed-phase system is ideally suited to spectroscopic investigations of the quantum nature of isomerization.

Direct conversion of molecules between their isomeric forms requires methods to reorganize bonds between constituent atoms. Such methods include thermal activation, laser-stimulated excitation (*1*–*4*), and electron-stimulated excitation (*5*–*7*). Understanding the quantum nature of isomerization is still a missing cornerstone in chemical science, as transitions between the quantum states involved in isomerization have never been detected. Stimulated emission pumping spectroscopy (*8*, *9*) has been used to examine the eigenstates of gas-phase systems capable of undergoing 1,2-hydrogen transfer reactions: e.g., HCN ⇌ CNH (*10*–*12*), HC≡CH ⇌ :C=CH_2 (*13*, *14*), and HCP ⇌ CPH (*15*). Yet even for these systems, it is challenging to detect quantum states from both isomers. Up to now, the most detailed quantum-state–resolved study employed high-resolution photoelectron spectroscopy to probe the HC≡CH ⇌ :C=CH_2 isomerization reaction and showed that the eigenstates of the in-plane rocking mode of vinylidene have appreciable acetylenic character (*16*). For symmetric systems that resemble chemical isomerization, such as the geared tunneling motion of the hydrogen-bonded HF dimer, HF···HF ⇌ FH···FH, delocalized states can be unambiguously identified from tunneling splitting (*17*).

Despite advances in understanding the vibrational character of these double-well systems (*18*, *19*), isomerization requires interactions with the environment that induce transitions between states. Hence, it would be desirable to extend quantum-state–resolved spectroscopy to temporally evolving systems in condensed phases. Unfortunately, the quantum states of condensed-phase systems generally cannot be spectroscopically resolved, and the theory needed for comparisons to experiment is much more demanding than that for small isolated molecules. We recently reported infrared emission spectra from monolayers of CO adsorbed at a NaCl(100) surface (*20*, *21*) using a spectrometer based on a superconducting nanowire single-photon detector (SNSPD) (*22*). Infrared laser excitation produced vibrationally excited CO by vibrational energy pooling (*23*), which could be accurately described by a kinetic Monte Carlo simulation (*21*). The interactions of the CO molecule with the NaCl lattice were described by a Sommerfeld ground-wave limit in which energy flow to the surface is dominated by electrodynamic interactions instead of the anharmonic interatomic forces that are normally much more important (*21*). These findings reflect the importance of electrostatic interactions in this system.

Here we present quantum-state–resolved infrared spectroscopy of two orientational isomers of a monolayer of CO on NaCl(100) observed in both absorption and emission. The ground-state orientation exhibits a short C–Na distance with the CO bond axis close to the surface normal; a less stable orientational isomer has a short O–Na bond with the bond axis tilted farther from the surface normal. Hereafter, we refer to these species as C-down and O-down, respectively. Vibrational energy pooling produces CO adsorbates with energies up to 6 eV, leading to infrared emission from well-resolved quantum states of both isomers. In fact, infrared laser excitation converts a substantial fraction of C-down to O-down. The lifetime of back-conversion to the C-down structure is short ($\lesssim 10^2$ s) at a surface temperature of 7 K. If we bury this monolayer under a weakly interacting CO overlayer, the lifetime of the O-down isomer becomes indefinite. From these data, we derived vibrational constants for both isomers in the monolayer and the buried monolayer. The shifts in the vibrational constants of the two orientational isomers referenced to the isolated gas-phase CO molecule obey a simple electrostatic model

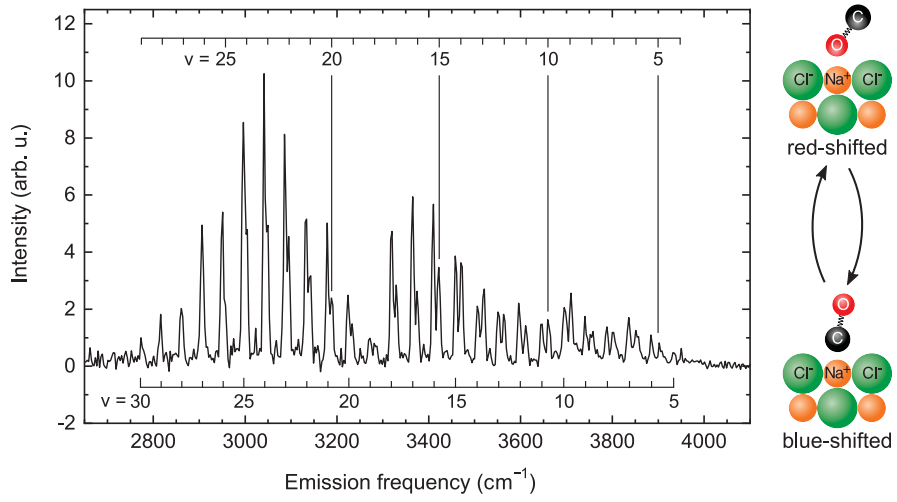

Fig. 1. Dispersed fluorescence spectrum from a monolayer of CO undergoing energy pooling. Two vibrational progressions shown by combs obey the simple anharmonic oscillator formula of Eq. 4, allowing derivation of precise vibrational constants for both progressions. One progression represents an anharmonic oscillator with blue-shifted frequencies compared with those of gas-phase CO; the second progression appears with red-shifted frequencies. The blue- and red-shifted oscillators are assigned to orientational isomers of CO at the NaCl interface, atomic scale representations of which are shown. Only overtone emission ($\Delta v = -2$) is shown, and the emission signal is integrated during the initial 200 μs after laser excitation. arb. u., arbitrary units.

[1]Institute for Physical Chemistry, University of Göttingen, Tammannstr. 6, 37077 Göttingen, Germany. [2]Department of Dynamics at Surfaces, Max-Planck Institute for Biophysical Chemistry, Am Faßberg 11, 37077 Göttingen, Germany. [3]National Institute of Standards and Technology, Boulder, CO 80305, USA. [4]International Center for Advanced Studies of Energy Conversion, Georg-August University of Göttingen, Tammannstraße 6, 37077 Göttingen, Germany.
*Present address: State Key Laboratory of Molecular Reaction Dynamics, Dalian Institute of Chemical Physics, Chinese Academy of Sciences, Dalian, Liaoning 116023, People's Republic of China.
†Corresponding author. Email: awodtke@mpibpc.mpg.de

that also describes the stable structures of the two isomers.

Figure 1 shows a section of the dispersed infrared fluorescence spectrum in the region of the first overtone obtained after pulsed IR excitation of the $^{13}C^{18}O(v = 0 \rightarrow 1)$ transition in a $^{13}C^{18}O$ monolayer sample. A process of rapid vibrational energy pooling leads to infrared emission from a manifold of vibrationally excited states of CO between v = 4 and 30. Populating vibrationally excited states results first from a sequence of energy transfer processes shown in Eq. 1.

$$\begin{aligned} &CO(1) + CO(1) \rightarrow CO(2) + CO(0) + \Delta\varepsilon(2) \\ &CO(2) + CO(1) \rightarrow CO(3) + CO(0) + \Delta\varepsilon(3) \\ &\qquad\vdots \qquad\qquad\qquad\vdots \\ &CO(v) + CO(1) \rightarrow CO(v+1) + CO(0) + \Delta\varepsilon(v+1) \end{aligned} \quad (1)$$

Here the integers represent CO's vibrational quantum number, v. These processes collect or "pool" vibrational energy into a fraction of the CO sample, eventually depleting the laser-prepared CO(v = 1) population. The highest value of v reached by these processes occurs when $\Delta\varepsilon(v)$—the energy release, which increases monotonically with v—exceeds the energy of the highest-frequency transverse phonon of NaCl (*21*). This occurs above v = 7. Slower but still important processes allow pooling to even higher vibrational states.

$$CO(n) + CO(m) \rightarrow CO(n+1) + CO(m-1) + \Delta\varepsilon(n,m) \quad (2)$$

Again, only those processes in which $\Delta\varepsilon(n,m)$ is less than the highest transverse phonon energy are important; m and n are between about 7 and 25. The larger average distance between these molecules reduces the rate of pooling.

With the use of an improved SNSPD-based spectrometer (*24*), two spectral progressions were resolved and assigned according to the combs of Fig. 1. We fit these two vibrational progressions using an energy expression for a harmonic oscillator with two anharmonic corrections

$$E(v) = hc\omega_e(v+1/2) - hc\omega_e x_e(v+1/2)^2 + hc\omega_e y_e(v+1/2)^3 \quad (3)$$

where h is Planck's constant, c is the speed of light, ω_e is the harmonic frequency, and $\omega_e x_e$ and $\omega_e y_e$ are anharmonic constants. The anharmonic nature of the C–O bond leads to an increasing shift of the overtone emission wave number, $\tilde{\nu}$, to lower values with increasing vibrational quantum number as can be seen from Eq. 4

$$\tilde{\nu} = \frac{1}{\lambda} = \frac{E(v) - E(v-2)}{hc} = 2\omega_e + (-4v+2)\omega_e x_e + (6v^2 - 6v + 7/2)\omega_e y_e \quad (4)$$

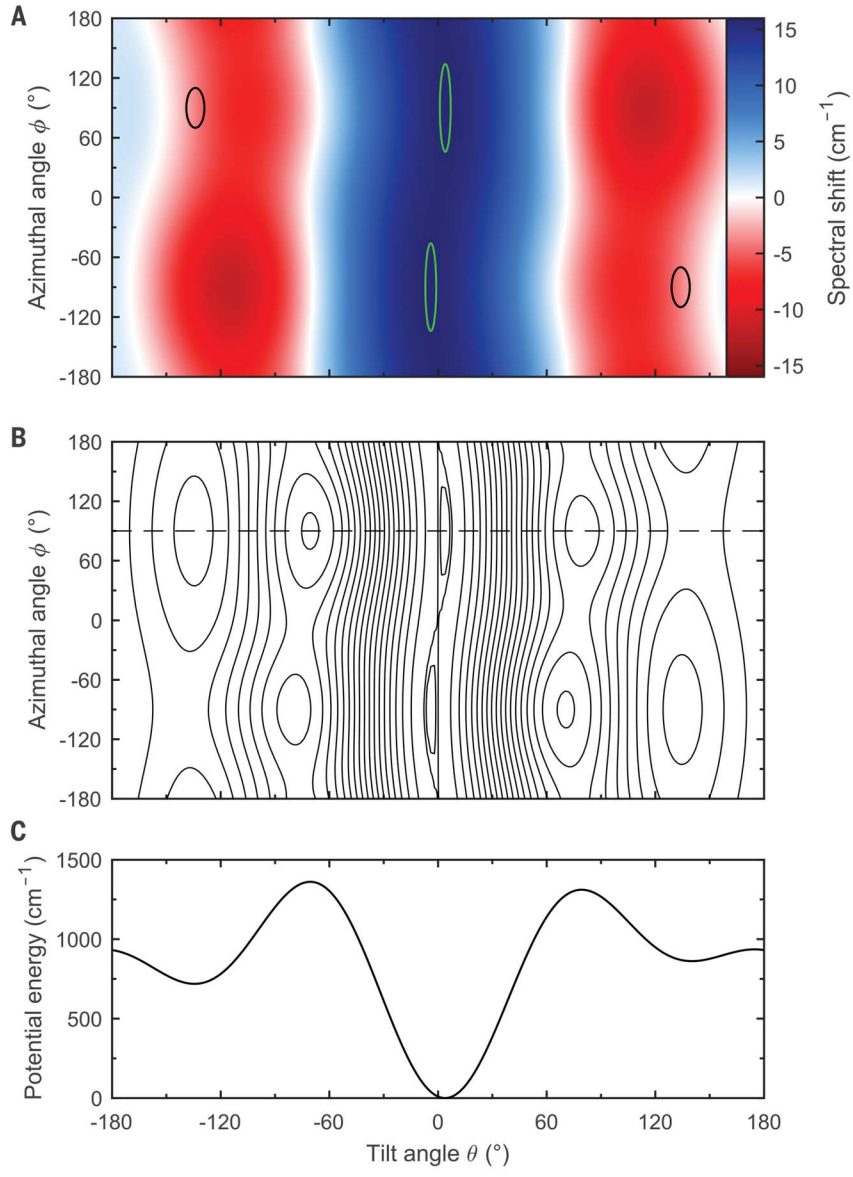

Fig. 2. Calculated dependence of the spectral frequency shift on the molecular orientation. (**A**) Changing the orientation of CO at NaCl results in frequency shifts due to electrostatic interactions with its surroundings. This spectral shift is calculated explicitly for the v = 0 → 1 transition. Green ovals indicate global minima on the electrostatic potential for CO(v = 0) with a C-down orientation. Black ovals indicate local minima for the O-down structure separated by a barrier much larger than k_BT (k_B, Boltzmann constant; T, temperature). Minima indicated by the same color correspond to identical orientations. The model predicts a blue shift for the C-down structure (+15.9 cm^{-1}) and a red shift for the O-down structure (−3.9 cm^{-1}). All shifts in wave number are relative to the isolated gas-phase molecule. (**B**) Vibrationally adiabatic electrostatic potential surface for the rotation of a single CO(v = 0) molecule in the monolayer structure. The contour lines show multiples of 75 cm^{-1}. Contour lines for 5 and 10 cm^{-1} have been added around $\theta = 0°$ to illustrate the shallow global minimum. (**C**) Cut through the potential surface at $\phi = 90°$, as indicated by the dashed line in (B).

where λ is the emission wavelength. The fitting procedure leads to precise values of ω_e, $\omega_e x_e$, and $\omega_e y_e$ for both spectral progressions. Table S1 displays these vibrational constants and extrapolated fundamental frequencies, along with reported values for gas-phase $^{13}C^{18}O$. The fundamental frequencies of the two emitters are shifted from that of the gas-phase molecule, but in opposite directions (+7.6 and −9.3 cm^{-1}). The harmonic frequencies ω_e show similar shifts, and $\omega_e x_e$ and $\omega_e y_e$ are slightly increased for both emitters.

The changes in the spectroscopic constants can be understood as a perturbation of the gas-phase molecule due to electrostatic interactions with its environment. A CO molecule

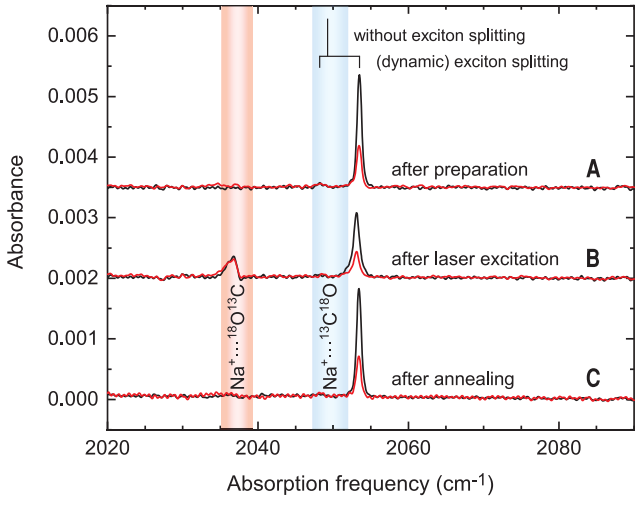

Fig. 3. Polarization-dependent FTIR spectrum of the two emitters in a buried monolayer. (**A**) The $^{13}C^{18}O$ monolayer was prepared on NaCl(100) and covered with ~100 monolayers of $^{12}C^{16}O$. Similar to the bare monolayer, the C-down structure shows a doublet with frequencies at 2048.2 and 2053.5 cm^{-1} due to vibrational exciton splitting. The splitting and the estimated frequency without splitting, as it would appear in emission, are indicated above the peaks (*24*). (**B**) The same sample has been irradiated with an infrared laser, inducing vibrational energy pooling in the buried $^{13}C^{18}O$ monolayer. The C-down absorption is reduced in intensity and a new absorption appears red-shifted by ~15 cm^{-1}, consistent with the prediction of the electrostatic model presented in Fig. 2. The red and blue bands indicate the positions of the $^{13}C^{18}O(v = 0 \rightarrow 1)$ transition, as predicted from the vibrational constants of table S1 derived from the infrared emission spectrum in fig. S3. The vertical line labeled "without exciton splitting" should be compared to the blue band. (**C**) FTIR spectrum obtained after annealing the sample to 22 K for 20 min. The O-down isomer has been converted back to the C-down structure. For all three curves, black and red spectra were recorded with a p- and s-polarized light source, respectively, and the effective resolution is ~0.7 cm^{-1}. Small absorption features due to impurities in the overlayer have been subtracted from all three spectra.

in vibrational state v will exhibit first-order energy corrections described by

$$E^{(1)} = f(\vartheta,\phi)F\mu_{vv} + g(\vartheta,\phi)\frac{\partial F}{\partial z}\,\Theta_{vv} + h(\vartheta,\phi)\frac{\partial^2 F}{\partial z^2}\Omega_{vv} + \cdots \quad (5)$$

when interacting with the local electric field, F, at a distance z from the NaCl(100) surface. Here, μ_{vv}, Θ_{vv}, and Ω_{vv} are the expectation values of the dipole, quadrupole, and octopole moments of CO in the vibrational state v. $f(\vartheta,\phi)$, $g(\vartheta,\phi)$, and $h(\vartheta,\phi)$ describe the orientation dependence of the interactions. As in Eq. 3, the expectation values of the multipole moments can be represented as a power series in $(v+1/2)$. For a given orientation, linear terms in $(v+1/2)$ give rise to a shift in ω_e, whereas quadratic and cubic terms lead to shifts in $\omega_e x_e$ and $\omega_e y_e$, respectively. Therefore, the emission frequencies of vibrational states below $v = 5$, for which the multipole moments are well described by a linear function (table S3), should show the same shift relative to the gas-phase frequencies. In fact, the experimental frequency shifts for $v \lesssim 10$ are identical within the uncertainty of the measured peak positions. For higher vibrational states, electrostatically induced changes in the anharmonic constants, $\omega_e x_e$ and $\omega_e y_e$, produce additional contributions to the frequency shifts. Unfortunately, accurate values of μ_{vv}, Θ_{vv}, and Ω_{vv} are not available for such high states, and this prevents a meaningful comparison of the experimentally observed frequencies with the predictions from an electrostatic model. Therefore, in the following analysis we restrict such comparisons to the observed fundamental frequency shift, where anharmonic contributions can be neglected.

The blue and red shifts of the fundamental frequencies from the gas-phase value are a direct result of the two emitters exhibiting different orientations on the NaCl surface. To envision this, consider the dipolar contribution to the interaction with the local electric field of the surface for the C-down molecule. In this case, the interaction is attractive, but because $|\mu_{00}|$ is greater than $|\mu_{11}|$, the $v = 0$ state is more stabilized by the interaction than is the $v = 1$ state—this gives rise to a blue-shifted transition. For the O-down molecule, the interaction is repulsive and, for the same reason, the $v = 1$ level is less destabilized than the $v = 0$ level—this gives rise to a red shift.

All multipole interactions with the surface and the neighboring CO molecules must be considered to correctly obtain the frequency shift. We have constructed an electrostatic model of the frequency shift including dipole, quadrupole, and octopole contributions (*24*). The calculated fundamental frequency shifts depend on two orientational angles (Fig. 2A). In this model, the CO bond of the C-down molecule is nearly normal to the surface with a tilt angle $\theta = 4°$ (Fig. 2, B and C). The O-down molecule is found at $\theta = 134°$ (i.e., the CO bond is tilted by 46° from the surface normal). The calculated frequency shifts of +15.9 and −3.9 cm^{-1} for the C-down and O-down isomer, respectively, as well as the total frequency splitting are in good qualitative agreement with the experimental shifts of +7.6 and −9.3 cm^{-1}. A similar positive offset is observed for the frequency shift of an isolated CO molecule adsorbed on NaCl (*24*). This analysis shows that both emitters are perturbed gas-phase CO molecules, altered by their electrostatic interactions with the NaCl surface and nearby CO molecules, and that they result from different orientational isomers.

Although only the C-down species is excited to $v = 1$ initially, the vibrational levels of both orientational isomers are close in energy and, thus, energy transfer processes as in Eqs. 1 and 2 are also possible between molecules in different orientations. Assuming that the total vibrational energy is evenly distributed between C-down and O-down, a crude estimate of the steady-state fraction of O-down molecules (46%) can be derived from the average intensity ratio between equal vibrational states in Fig. 1. The O-down isomer in the monolayer does not convert back to the C-down structure during the ~10 ms in which infrared fluorescence is observed. But its lifetime is sufficiently short that an absorption or laser-induced fluorescence (LIF) excitation spectrum for the O-down species could not be obtained (we require minutes to move the sample into position for an absorption experiment or to attempt to record a LIF spectrum of the O-down isomer).

The O-down isomer can, however, be stabilized indefinitely if we perform the vibrational energy pooling experiment on a buried monolayer. Using pulsed molecular beam dosing (fig. S1B), a $^{13}C^{18}O$ monolayer sample was prepared on NaCl(100), and a $^{12}C^{16}O$ overlayer was deposited on top of it. Just as for the uncovered monolayer, we observe vibrational energy pooling and infrared emission spectra that show two emitters (C-down and O-down) when the infrared laser is used to selectively excite $^{13}C^{18}O(v = 0 \rightarrow 1)$ in the buried monolayer (fig. S3).

The long lifetime of O-down CO in the buried monolayer allows us to obtain its infrared absorption spectrum. Figure 3 shows three Fourier transform infrared (FTIR) absorption spectra obtained with various treatments of the buried monolayer. Initially after sample preparation, only the C-down species is present with absorption features at 2048.2 and 2053.5 cm^{-1}, blue-shifted from the CO gas-phase absorption at 2043.7 cm^{-1}. The strong polarization dependence of the absorption results from the geometry of the experiment and the near-normal orientation of the CO bond in the adsorbed species (*25*, *26*). After ~6000 pulses of IR light have irradiated the sample and induced vibrational energy pooling, the absorption of C-down

is reduced and a new absorption is seen at 2037 cm^{-1}, red-shifted from the gas-phase value. The red and blue bands of Fig. 3 indicate the predicted positions of the $^{13}C^{18}O(v = 0 \rightarrow 1)$ transition, as determined from the vibrational constants of table S1 derived from the infrared emission spectrum in fig. S3. The lack of a polarization dependence for the O-down absorption indicates a tilt angle, θ, consistent with the predictions of the electrostatic model of Fig. 2. Finally, Fig. 3C shows the full recovery of the C-down isomer and loss of the O-down isomer when the sample has been annealed to 22 K for ~20 min.

In this work, we observed infrared emission and absorption spectra of two orientational isomers of CO adsorbed to NaCl(100) and discovered how the C-down isomer can be converted to the less stable O-down isomer through infrared laser excitation. Our findings emphasize that, in contrast to most previously studied systems that exhibit a single orientation necessary to form a chemical bond between the molecule and the surface, adsorbates bound by electrostatic interactions exhibit more diverse adsorption geometries that are more easily interconverted, owing to the vibrational dependence of the electrostatic interactions. Ground-state CO has a dipole oriented as $C^{\delta-}O^{\delta+}$ (table S3), which leads to an electrostatic bond with the C atom adjacent to a Na^+ ion. In the high vibrational states observed in this work, the dipole moment reverses sign ($C^{\delta+}O^{\delta-}$), contributing a force that can rotate the molecule to the O-down configuration. Yet this simplified picture, although intuitively appealing, neglects a number of potentially important effects. If a full-dimensional potential energy surface can be calculated, as has been accomplished for other condensed-phase systems (*27*), quantum dynamics of isomerization can be studied with theory and compared to experimental results, leading to a deeper understanding of this phenomenon.

Many future experiments are now possible. Relevant to better understanding the quantum nature of isomerization, the lifetime of the O-down interconversion to C-down can be directly measured, and state-to-state pathways from one isomer to another can be mapped using time-resolved pump-probe methods. Beyond this, other examples of switchable adsorbates are also likely to be found in the future, because systems dominated by weak electrostatic interactions are common. Candidates for future study include CO on other salt crystals and CO on insulating solids such as hydrogen-terminated diamond, hydrogen-terminated silicon, and metal oxides. Because substrate variation can strongly influence both the vibrational energy pooling and the relative stability of the two isomers, controlled switching between the isomers may also be achievable. Electronic excitation of CO to the $a^3\Pi$ state also results in sudden changes in both the sign and magnitude of the dipole moment (*28*) that likely lead to reorientation and intersystem crossing to the ground state. The use of electronic excitation to induce isomerization in such condensed-phase systems promises another experimental approach to quantum-state–resolved isomerization. Such detailed experimental studies provide a fruitful breeding ground for new and accurate theoretical studies of condensed-phase quantum isomerization.

REFERENCES AND NOTES

1. P. Nogly *et al.*, *Science* **361**, eaat0094 (2018).
2. V. I. Prokhorenko *et al.*, *Science* **313**, 1257–1261 (2006).
3. T. Kobayashi, T. Saito, H. Ohtani, *Nature* **414**, 531–534 (2001).
4. M. Tsuda, M. Glaccum, B. Nelson, T. G. Ebrey, *Nature* **287**, 351–353 (1980).
5. T. Kudernac *et al.*, *Nature* **479**, 208–211 (2011).
6. A. Safiei, J. Henzl, K. Morgenstern, *Phys. Rev. Lett.* **104**, 216102 (2010).
7. B. Y. Choi *et al.*, *Phys. Rev. Lett.* **96**, 156106 (2006).
8. C. E. Hamilton, J. L. Kinsey, R. W. Field, *Annu. Rev. Phys. Chem.* **37**, 493–524 (1986).
9. C. Kittrell *et al.*, *J. Chem. Phys.* **75**, 2056–2059 (1981).
10. X. M. Yang, C. A. Rogaski, A. M. Wodtke, *J. Opt. Soc. Am. B* **7**, 1835 (1990).
11. D. M. Jonas, X. M. Yang, A. M. Wodtke, *J. Chem. Phys.* **97**, 2284–2298 (1992).
12. M. Silva, R. Jongma, R. W. Field, A. M. Wodtke, *Annu. Rev. Phys. Chem.* **52**, 811–852 (2001).
13. M. P. Jacobson, R. W. Field, *J. Phys. Chem. A* **104**, 3073–3086 (2000).
14. Y. Q. Chen, D. M. Jonas, J. L. Kinsey, R. W. Field, *J. Chem. Phys.* **91**, 3976–3987 (1989).
15. H. Ishikawa *et al.*, *Annu. Rev. Phys. Chem.* **50**, 443–484 (1999).
16. J. A. DeVine *et al.*, *Science* **358**, 336–339 (2017).
17. T. R. Dyke, B. J. Howard, W. Klemperer, *J. Chem. Phys.* **56**, 2442–2454 (1972).
18. J. M. Bowman, B. Gazdy, J. A. Bentley, T. J. Lee, C. E. Dateo, *J. Chem. Phys.* **99**, 308–323 (1993).
19. M. Joyeux, S. C. Farantos, R. Schinke, *J. Phys. Chem. A* **106**, 5407–5421 (2002).
20. L. Chen *et al.*, *Opt. Express* **26**, 14859–14868 (2018).
21. L. Chen *et al.*, *Science* **363**, 158–161 (2019).
22. L. Chen *et al.*, *Acc. Chem. Res.* **50**, 1400–1409 (2017).
23. H. C. Chang, G. E. Ewing, *Phys. Rev. Lett.* **65**, 2125–2128 (1990).
24. See supplementary materials.
25. D. Schmicker, J. P. Toennies, R. Vollmer, H. Weiss, *J. Chem. Phys.* **95**, 9412–9415 (1991).
26. J. Heidberg, E. Kampshoff, M. Suhren, *J. Chem. Phys.* **95**, 9408–9411 (1991).
27. Y. Wang, B. C. Shepler, B. J. Braams, J. M. Bowman, *J. Chem. Phys.* **131**, 054511 (2009).
28. B. G. Wicke, R. W. Field, W. Klemperer, *J. Chem. Phys.* **56**, 5758–5770 (1972).

ACKNOWLEDGMENTS

Funding: We acknowledge support from the MPS-EPFL joint international Center in Molecular Nanoscience and Technology. **Author contributions:** J.A.L. performed infrared emission spectroscopy experiments, analyzed data, and constructed the electrostatic model. A.C. performed infrared emission spectroscopy experiments and analyzed data. L.C. and D.S. built and commissioned the instrument. V.B.V. developed the SNSPDs used in this work. A.M.W. conceived the experiment and wrote the first draft of the paper. A.M.W., V.B.V., D.S., J.A.L., and A.C. also participated in writing and revising the paper. **Competing interests:** None declared. **Data and materials availability:** All data needed to evaluate the conclusions in the paper are present in the paper or the supplementary materials.

SUPPLEMENTARY MATERIALS

science.sciencemag.org/content/367/6474/175/suppl/DC1
Materials and Methods
Supplementary Text
Figs. S1 to S4
Tables S1 to S3
References (*29*–*40*)

1 September 2019; accepted 13 November 2019
10.1126/science.aaz3407

Observation of an isomerizing double-well quantum system in the condensed phase

Jascha A. Lau, Arnab Choudhury, Li Chen, Dirk Schwarzer, Varun B. Verma and Alec M. Wodtke

Science **367** (6474), 175-178.
DOI: 10.1126/science.aaz3407

Upside-down molecules on a salt surface

The quantum states of molecules are usually measured in gas-phase studies to minimize collisions that would blur the spectra. However, for carbon monoxide (CO) molecules adsorbed on a NaCl(100) surface, infrared emission from even high vibrational states can be resolved. In quantum-state resolved spectra, Lau *et al.* found that infrared-laser excitation of a monolayer of CO adsorbed on NaCl(100) forms an isomer in which CO binds to Na^+ through its O atom in an upside-down configuration (see the Perspective by Wu). These results could be understood with a simple vibrationally adiabatic electrostatic theory, making this system convenient for studies of the isomerization chemistry.

Science, this issue p. 175; see also p. 148